Dielectrophoretic Concentration and Separation of Live and Dead Bacteria in an Array of Insulators

Blanca H. Lapizco-Encinas,[†] Blake A. Simmons,[‡] Eric B. Cummings,[†] and Yolanda Fintschenko*,[†]

Microfluidics Department, Sandia National Laboratories, P.O. Box 969, MS 9951, Livermore, California 94551, and Materials Chemistry Department, Sandia National Laboratories, P.O. Box 969, MS 9403, Livermore, California 94551

Insulator-based (electrodeless) dielectrophoresis (iDEP) is an innovative approach in which the nonuniform electric field needed to drive DEP is produced by insulators, avoiding problems associated with the use of electrodes. Live and dead *Escherichia coli* were concentrated and selectively released by applying stepped DC voltages across a microchannel containing an array of insulating posts etched in glass. The only electrodes present were two platinum wires placed in the inlet and outlet reservoirs, producing mean electric fields of up to 200 V/mm across the insulators. The cells were labeled with Syto 9 and propidium iodide and imaged through a fluorescent microscope. Cell trapping and release were controlled by modifying the relative responses of electrokinesis and DEP by adjusting the magnitude of the applied voltage. Dead cells were observed to have significantly lower dielectrophoretic mobility than live cells, whereas the electrokinetic mobilities of live and dead cells were indistinguishable. The locations of the bands of differentially trapped cells were consistent with predictions. In addition, cells were selectively trapped and concentrated against backgrounds of 1- and 0.2-μm carboxylate-modified polystyrene particles. This first application of iDEP for simultaneous live/dead bacteria separation and concentration illustrates its potential as a front-end method for bacterial analysis.

Water analysis, in which one pathogenic bacterium per liter of water is of concern, is an example of an application that requires high fluid throughput and the ability to concentrate particles. Because of the comparatively large concentration of dead and inert particles in water samples, selective concentration is desirable. Conventional analysis methods, such as mechanical filtration, involve a lengthy culture step. By utilizing insulator-based (electrodeless) dielectrophoresis (iDEP), selective concentration can be achieved in a single automated device. Whereas iDEP has been demonstrated with polystyrene beads, DNA, and yeast cells,[1−6] it has not previously been reported with live and dead bacterial cells.[7] The great potential for the application of iDEP for the selective concentration of bacteria from water motivates these bacterial studies.

A number of methods exist to separate and concentrate bacteria, including the ubiquitous techniques of filtration and centrifugation. However, electric field-based separation methods are of interest because of their potential for automation, miniaturization, and massive parallelization. A number of studies have been carried out using CE for the separation of bacteria and viruses.[8−24] By employing CE, the intact microbes can be separated on the basis of their characteristic charge-to-mass ratio, which varies with pH, solution composition, ionic strength, and temperature.[9] However, CE cannot necessarily distinguish between live and dead organisms on the basis of a difference in migration time. Armstrong et al.[8−13,25] have described CE of a variety of microorganisms. Their studies included the determination of cell viability for *Bifidobacterium infantis*, *Lactobacillus acidophilus*, and *Sac-*

* Corresponding author. Phone: (925) 294-4920. Fax: (925) 294-3020. E-mail: yfintsc@sandia.gov.

[†] Microfluidics Department.

[‡] Materials Chemistry Department.

(1) Cummings, E.; Singh, A. *Proc. SPIE- Int. Soc. Opt Eng*, Santa Clara, CA, 2000; 164−173.

(2) Cummings, E.; Singh, A. *Anal. Chem*. **2003**, *75*, 4724−4731.

(3) Cummings, E. B. 32nd AIAA Fluid Dynamics Conference and Exhibit 2002; Proc. 32nd AIAA, St. Louis, MO 2002, 2002−3193.

(4) Chou, C.; Tegenfeldt, J.; Bakajin, O.; Chan, S.; Cox, E.; Darnton, N.; Duke, T.; Austin, R. *Biophys. J.* **2002**, *83*, 2170−2179.

(5) Zhou, G.; Imamura, M.; Suehiro, J.; Hara, M. *Proc. IEEE: 37th Ann. Meet. IEEE Indust. Appl. Soc.*, Pittsburgh, PA, 2002; 1404−1411.

(6) Suehiro, J.; Zhou, G.; Imamura, M.; Hara, M. *Proc. IEEE: Ann. Meet. IEEE Indust. Appl. Soc.*, Pittsburgh, PA 2003; 1514−1521.

(7) Gascoyne, P.; Vykoukal, J. *Electrophoresis* **2002**, *23*, 1973−1983.

(8) Armstrong, D.; Schulte, G.; Schneiderheinze, J.; Westenberg, D. *Anal. Chem*. **1999**, *71*, 5465−5469.

(9) Armstrong, D.; He, L. *Anal. Chem*. **2001**, *73*, 4551−4557.

(10) Armstrong, D.; Schneiderheinze, J.; Kullman, J.; He, L. *FEMS Microbiol. Lett*. **2001**, *194*, 33−37.

(11) Armstrong, D. W.; Girod, M.; He, L.; Rodriguez, M. A.; Wei, W.; Zheng, J.; Yeung, E. S. *Anal. Chem*. **2002**, *74*, 5523−5530.

(12) Girod, M.; Armstrong, D. W. *Electrophoresis* **2002**, *23*, 2048−2056.

(13) Schneiderheinze, J. M.; Armstrong, D. W.; Schulte, G.; Westenberg, D. J. *FEMS Microbiol. Lett.* **2000**, *189*, 39−44.

(14) Cabrera, C. R.; Yager, P. *Electrophoresis* **2001**, *22*, 355−362.

(15) Kenndler, E.; Blaas, D. *TRAC-Trends Anal. Chem*. **2001**, *20*, 543−551.

(16) Buszewski, B.; Szumski, M.; Klodzinska, E.; Dahm, H. *J. Sep. Sci*. **2003**, *26*, 1045−1049.

(17) Kourkine, I.; Ristic-Petrovic, M.; Davis, E.; Ruffolo, C.; Kapsalis, A.; Barron, A. *Electrophoresis* **2003**, *24*, 655−661.

(18) Li, P.; Harrison, D. *Anal. Chem*. **1997**, *69*, 1564−1568.

(19) Pfetsch, A.; Welsch, T. *Fresenius' J. Anal. Chem*. **1997**, *359*, 198−201.

(20) Mehrishi, J.; Bauer, J. *Electrophoresis* **2002**, *23*, 1984−1994.

(21) Radko, S.; Chrambach, A. *Electrophoresis* **2002**, *23*, 1957−1972.

(22) Torimura, M.; Ito, S.; Kano, K.; Ikeda, T.; Esaka, Y.; Ueda, T. *J. Chromatogr., B* **1999**, *721*, 31−37.

(23) Sonohara, R.; Muramatsu, N.; Ohshima, H.; Kondo, T. *Biophys. Chem*. **1995**, *55*, 273−277.

(24) Glynn, J.; Belongia, B.; Arnold, R.; Ogden, K.; Baygents, J. *Appl. Environ. Microbiol.* **1998**, *64*, 2572−2577.

(25) Armstrong, D. W.; Schneiderheinze, J. M. *Anal. Chem*. **2000**, *72*, 4474−4476.

10.1021/ac034804j CCC: $27.50
Published on Web 00/00/0000

charomyces cerevisiae, in which the results indicated the live and dead cells had indistinguishable migration times.[9] Migration times for live and dead *L. acidophilus* cells were also reported as effectively identical.[10] The development of methods and devices for the continuous concentration of bacteria using a variety of electrokinetic techniques, including zone electrophoresis and isoelectric focusing, is nascent but growing.[14,18,22]

Field-flow fractionation (FFF) has also been used alone and in conjunction with dielectrophoresis (DEP) for the separation and concentration of cells.[26−29] In DEP−FFF the particles are levitated at different heights from the wall of a separation chamber, reaching higher positions in the parabolic velocity profile of the liquid flowing through the chamber. Particles are eluted from the chamber in decreasing order of their velocities.[30,31] Gascoyne et al.[32,33] utilized a DEP−FFF system to separate mammalian cells. Cells were eluted from the DEP−FFF system as a function of the frequency and voltage of the applied electric field and their dielectric characteristics.

Dielectrophoresis, a phenomenon first described by Pohl in 1951, is the movement of particles caused by polarization effects in a nonuniform electric field.[34−36] DEP can take place in either direct (DC) or alternating (AC) electric fields.[37]

A material that passes displacement or conduction currents in response to an electric field is at lower electrostatic potential where that field is higher. A mobile particle, therefore, experiences a force toward regions of high electric field intensity. The resulting motion is called dielectrophoresis.[36,38,39] Particles having a higher polarizability than their immersion medium exhibit positive dielectrophoresis: motion toward regions of greater field intensity under this unbalanced electrostatic force. Conversely, particles having a lower conductivity than their immersion medium exhibit negative dielectrophoresis: motion away from regions of high electric field intensity as the medium displaces them from the high-field regions.[36,38,39]

The utility of DEP for the separation of cells was demonstrated first by Pohl and others.[38,40,41] Initial studies of cells by DEP employed electrodes of different shapes in order to produce nonuniform electric fields. Pohl et al.[36,38,40,41] used pin−plate and pin−pin electrodes to separate live and dead yeast cells and achieved the collection of yeast cells on the electrodes. Recently, due to the availability of microfabrication techniques, DEP applications have been carried out using arrays of microelectrodes and AC electric fields. The minute dimensions of microelectrodes permit high electric field intensity at lower voltages, driving DEP with less heating of the system.[39,42] The large majority of the recent DEP studies reported have used thin-film electrode arrays (e.g., polynomial, interdigitated, sawtooth) fabricated in channels/flow cells with AC fields to generate nonuniform electric fields.[32,33,43−54] Other studies have used three-dimensional electrode cages to capture and handle single cells and particles.[55−60] AC electric fields are used to eliminate electroosmosis and gas generation.[2]

Markx et al.[43,44] characterized and separated viable and nonviable yeast, Gram positive, and Gram negative bacteria by employing polynomial and interdigitated microelectrodes. In 1996, Markx et al.[45] also carried out dielectrophoretic separation of bacteria on interdigitated microelectrodes by varying the conductivity of the medium. Medoro et al.[55−57] developed a cell manipulator device by using 3D structures of electrodes. Müller et al.[58] also developed a 3D microelectrode system for the handling and the caging of single cells and particles. Fiedler et al.[61] used a dielectrophoretic microdevice that contained a 3D cage that was used to trap latex particles and cells. Li and Bashir[46] separated live and heat-treated cells of *Listeria* on microfabricated interdigitated electrodes.

Suehiro et al.[6,62−65] and Zhou et al.[5] have used both electrode-based and insulator-based DEP to separate yeast cells; they used peristaltic pumps and have achieved flow rates up to 2.5 mL/min. They also demonstrated the concentration and manipulation of yeast cells using an AC field applied to a dual electrode cell filled

(26) Giddings, J. C. *Science* **1993**, *269*, 1456−1465.
(27) Lee, H.; Williams, S.; Wahl, K.; Valentine, N. *Anal. Chem.* **2003**, *75*, 2746−2752.
(28) Gascoyne, P.; Huang, Y.; Wang, X.; Yang, J.; Degasperis, G.; Wang, X. *Biophys. J.* **1996**, *70*, TU412.
(29) Gao, Y.-S.; Lorbach, S. C.; Blake, R. *J. Microcolumn Sep.* **1997**, *9*, 497−501.
(30) Markx, G.; Rousselet, J.; Pethig, R. *J. Liq. Chromatogr., Relat. Technol.* **1997**, *20*, 2857−2872.
(31) Pethig, R.; Markx, G. H. *Trends Biotechnol.* **1997**, *15*, 426−432.
(32) Yang, J.; Huang, Y.; Wang, X.; Becker, F.; Gascoyne, P. *Anal. Chem.* **1999**, *71*, 911−918.
(33) Wang, X.-B.; Yang, J.; Huang, Y.; Vykoukal, J.; Becker, F. F.; Gascoyne, P. R. C. *Anal. Chem.* **2000**, *72*, 832−839.
(34) Pohl, H. *Appl. Phys.* **1951**, *22*, 869−871.
(35) Jones, T. B. *Electromechanics of Particles*; Cambridge University Press: New York, 1995.
(36) Pohl, H. *Dielectrophoresis*; Cambridge University Press: Cambridge, 1978.
(37) Pohl, H. *Appl. Phys.* **1958**, *29*, 1182−1188.
(38) Crane, J.; Pohl, H. *J. Electrochem. Soc.* **1968**, *115*, 584−586.
(39) Betts, W. *Trends Food Sci. Technol.* **1995**, *6*, 51−58.
(40) Pohl, H.; Hawk, I. *Science* **1966**, *152*, 647−649.
(41) Pohl, H.; Crane, J. *Biophys. J.* **1971**, *11*, 711−727.
(42) Malyan, B.; Balachandran, W. *J. Electrostatics* **2001**, *51*, 15−19.
(43) Markx, G. H.; Huang, Y.; Zhou, X. F.; Pethig, R. *Microbiology-UK* **1994**, *140*, 585−591.
(44) Markx, G. H.; Talary, M. S.; Pethig, R. *J. Biotechnol.* **1994**, *32*, 29−37.
(45) Markx, G.; Dyda, P.; Pethig, R. *J. Biotechnol.* **1996**, *51*, 175−180.
(46) Li, H.; Bashir, R. *Sens. Actuators, B* **2002**, *86*, 215−221.
(47) Morgan, H.; Green, N. *J. Electrostatics* **1997**, *42*, 279−293.
(48) Green, N.; Morgan, H.; Milner, J. *J. Biochem. Biophys. Methods* **1997**, *35*, 89−102.
(49) Morgan, H.; Hughes, M.; Green, N. *Biophys. J.* **1999**, *77*, 516−525.
(50) Hughes, M.; Morgan, H.; Rixon, F.; Burt, J.; Pethig, R. *Biochim. Biophys Acta* **1998**, *1425*, 119−126.
(51) Hughes, M.; Morgan, H.; Rixon, F. *Eur. Biophys J. Biophys. Lett.* **2001**, *30*, 268−272.
(52) Hughes, M.; Morgan, H.; Rixon, F. *Biochim. Biophys Acta* **2002**, *1571*, 1−8.
(53) Betts, W.; Brown, A. *J. Appl. Microbiol.* **1999**, *85*, 201S−213S.
(54) Fuhr, G.; Glasser, H.; Muller, T.; Schnelle, T. *Biochim. Biophys. Acta* **1994**, *1201*, 353−360.
(55) Medoro, G.; Manaresi, N.; Tartagni, M.; Guerrieri, R. *Proc. IEEE: Int. Electron Devices Meet.*, San Francisco, CA, 2000; 415−418.
(56) Medoro, G.; Manaresi, N.; Leonardi, A.; Altomare, L.; Tartagni, M.; Guerrieri, R. *Proc. IEEE: Sensors*, Orlando, FL, 2002; 472−477.
(57) Medoro, G.; Manaresi, N.; Altomare, L.; Leonardi, A.; Tartagni, M.; Guerrieri, R. *Proc. Eurosensors XVI*, Prague, Czech Republic, 2002.
(58) Müller, T.; Gradl, G.; Howitz, S.; Shirley, S.; Schnelle, T.; Fuhr, G. *Biosens. Bioelectron.* **1999**, *14*, 247−256.
(59) Schnelle, T.; Muller, T.; Fiedler, S.; Shirley, S.; Ludwig, K.; Herrmann, A.; Fuhr, G.; Wagner, B.; Zimmermann, U. *Naturwissenschaften* **1996**, *83*, 172−176.
(60) Müller, T.; Fiedler, S.; Schnelle, T.; Ludwig, K.; Jung, H.; Fuhr, G. *Biotechnol. Tech.* **1996**, *10*, 221−226.
(61) Fiedler, S.; Shirley, S.; Schnelle, T.; Fuhr, G. *Anal. Chem.* **1998**, *70*, 1909−1915.
(62) Suehiro, J.; Pethig, R. *J. Phys. D: Appl. Phys.* **1998**, *31*, 3298−3305.
(63) Suehiro, J.; Noutomi, D.; Hamada, R.; Hara, M. *Proc. IEEE. 36th Ann. Meet. Indust. Appl. Soc.*, Chicago, IL 2001; 1950−1955.
(64) Suehiro, J.; Hamada, R.; Noutomi, D.; Shutou, M.; Hara, M. *J. Electrost.* **2003**, *57*, 157−168.
(65) Suehiro, J.; Noutomi, D.; Shutou, M.; Hara, M. *J. Electrost.* **2003**, *58*, 229−246.

with glass spheres.[5,6] In addition, they achieved selective detection of viable bacteria using a dielectrophoretic impedance method.[63]

The use of insulators rather than electrode arrays to produce a nonuniform electric field has a number of advantages. Insulators are less prone to fouling; that is, they generally retain their function despite surface changes. Insulators can be made more robust and chemically inert than metallic electrodes. Fabrication with solely insulating materials eliminates the metal deposition and patterning step required for electrode arrays. Additionally, a DC field can be used for solution and particle flow through the device by electrokinesis as well as dielectrophoretic trapping.

Insulator-based dielectrophoresis (iDEP) of latex particles with DC electrical fields was described by Cummings and Singh in 2000.[1] This method employs an array of insulating posts etched in a microchannel in order to create a nonuniform electric field. The posts are fabricated from an insulating material (e.g., glass or plastic). Only two electrodes are needed, at the solution inlet and outlet. The insulating posts modify the electric field distribution between the two electrodes, creating zones with relatively higher and lower field strengths.[1−3] DEP is of second order in the applied electric field. Electrokinesis is of first order in the applied electric field. Electrokinesis was used to flow the liquid and particles through the array of insulating posts. At low applied electric fields, DEP is negligible, as compared to electrokinesis. As the DC electric field strength is increased, trapping DEP occurs when the DEP force overcomes electrokinesis and other transport mechanisms. Under this regime, particles of interest are dielectrophoretically immobilized and can be significantly concentrated nearly to solid density while the solution and unaffected particles continue to flow past due to electrokinesis.[2] Cummings et al. described the theory and proof of concept of iDEP in DC fields using 200-nm polystyrene beads.[1−3]

Described here is the application of DC-iDEP for the selective concentration of live and dead bacteria. Insulating-post structures fabricated in glass were successfully used to simultaneously concentrate and separate live *Escherichia coli* in the presence of dead *E. coli* and inert particles using only DC fields. To the best of our knowledge, this is the first report of DC-iDEP for the simultaneous concentration and separation of live and dead bacteria.

THEORY

Theoretical Basis of Separation of Live and Dead Bacteria Cells. The dielectrophoretic force acting on a spherical particle can be described by eq 1,[35]

$$F_{\mathrm{DEP}} = 2\pi\epsilon_0\epsilon_{\mathrm{m}} r^3 Re[f(\tilde{\sigma}_{\mathrm{p}}, \tilde{\sigma}_{\mathrm{m}})]\nabla(\mathbf{E}\cdot\mathbf{E}) \qquad (1)$$

where ϵ_0 is the permittivity of free space, ϵ_{m} is the relative permittivity of the suspending medium, r is the radius of the particle, ($\mathbf{E}\cdot\mathbf{E}$) is the local electric field intensity, $\tilde{\sigma}_{\mathrm{p}}$ and $\tilde{\sigma}_{\mathrm{m}}$ are the complex conductivities of the particle and the medium respectively, and $f(\tilde{\sigma}_{\mathrm{p}}, \tilde{\sigma}_{\mathrm{m}})$ is the well-known Clausius−Mossotti (CM) factor that describes the electrostatic properties of an immersed spherical particle. At low frequency, because the dominant electrostatic effect is conduction, the real part of the CM factor depends solely on the conductivity of the particle and suspending medium. In this regime, the CM factor is most clearly expressed in terms of complex conductivities

$$\tilde{\sigma} = \sigma + i\omega\epsilon \qquad (2)$$

where σ is the real conductivity, ϵ is the relative dielectric constant, $i = \sqrt{-1}$, and ω is the angular frequency of the applied electric field, the CM factor becomes[35,66,67]

$$f(\tilde{\sigma}_{\mathrm{p}}, \tilde{\sigma}_{\mathrm{m}}) = \left[\frac{\tilde{\sigma}_{\mathrm{p}} - \tilde{\sigma}_{\mathrm{m}}}{\tilde{\sigma}_{\mathrm{p}} + 2\tilde{\sigma}_{\mathrm{m}}}\right] \qquad (3)$$

In many practical systems, at frequencies below 100 kHz, the CM factor can be approximated in terms of the real conductivities as[45,68]

$$f(\tilde{\sigma}_{\mathrm{p}}, \tilde{\sigma}_{\mathrm{m}}) = \left[\frac{\sigma_{\mathrm{p}} - \sigma_{\mathrm{m}}}{\sigma_{\mathrm{p}} + 2\sigma_{\mathrm{m}}}\right] \qquad (4)$$

As eq 1 shows, the dielectrophoretic force acting on a particle can be positive or negative, depending on the sign of the CM factor. If the conductivity of the particle is greater than the conductivity of the medium, then the particle will exhibit positive DEP, and vice versa. It has been reported that at low frequencies, the applied electric field is primarily dropped across the outer cellular membrane, and the cells behave as poorly conductive spheres. At higher frequencies, the applied field is able to penetrate into the cells, and the cells behave more as conductive spheres having the conductivity of the cells' interior.[31,35,43,46,69−72] Therefore, depending on the applied electric field (low-frequency AC, high-frequency AC or DC), different dielectrophoretic responses can be observed. The current study employed only DC electric fields; therefore, it is assumed that the dielectrophoretic response of the cells depended on the conductivity of the cell membranes.

The conductivity of a cell's interior can be as high as 1×10^3 μS/mm, since cells contain many ions and charged particulates. In contrast, the conductivity of cell membranes tends to be $\sim 10^{-4}$ μS/mm. When a cell dies, the cell membrane becomes permeable, and its conductivity can increase by a factor of 10^4. When using a DC electric field, one therefore expects live cells (membrane conductivity $\sim 10^{-4}$ μS/mm) to exhibit more negative DEP than dead cells (membrane conductivity ~ 1 μS/mm).[31] Therefore, under these conditions, the dielectrophoretic separation of live and dead cells should be possible due to the differences in the conductivity of their cell membranes. Table 1 shows the values of conductivities of the cell membranes, the cells as whole, the polystyrene particles, the suspending medium, and the CM factors for the cells and particles suspended in DI water. It is important

(66) Benguigui, L.; Lin, I. J. *J. Appl. Phys.* **1984**, *56*, 3294−3297.
(67) Morgan, H.; Green, N. G. *AC Electrokinetics: Colloids and Nanoparticles*; Research Studies Press LTD: Hertfordshire, England, 2003.
(68) Van Den Wal, A.; Minor, M.; Norde, W.; Zehnder, A. J. B.; Lyklema, J. *J. Colloid Interface Sci.* **1997**, *186*, 71−79.
(69) Carstensen, E. L.; Cox, H. A., Jr.; Mercer, W. B.; Natale, L. A. *Biophys. J.* **1965**, *5*, 289−300.
(70) Carstensen, E. L. *Biophys. J.* **1967**, *7*, 493−503.
(71) Burt, J.; Pethig, R.; Gascoyne, P. R. C.; Becker, F. *Biochim. Biophys. Acta* **1990**, *1034*, 93−101.
(72) Yunus, Z.; Mason, V.; Verduzco-Luque, C. E.; Markx, G. H. *J. Microbiol. Methods* **2002**, *51*, 401−406.

Table 1. Conductivity and Clausius−Mossotti Factors of Cells and Particles Suspended in DI Water

item	conductivity (μS/mm)	Clausius-Mossotti factor (DI water as suspending medium)
membrane of live cell[31]	1×10^{-4}	−0.50
membrane of dead cell[30]	1	−0.23
cytoplasm of live *E. coli* cell[43]	41.2	+0.85
polystyrene particles (557 nm)[74]	18.5	+0.71
DI water utilized[a]	2.25 ± 0.01	

[a] Our measurement performed with a Mettler Toledo MC126 conductivity meter.

to mention that the value shown for the polystyrene particles is for particles having a diameter of 557 nm. The particles utilized had diameters of 200 nm and 1 μm, respectively. The 200-nm particles are expected to have a conductivity value higher than the value reported in Table 1. The 1-μm particles are expected to have a conductivity value lower than the value reported in Table 1. This can be explained as follows: a particle conducts through its bulk by an amount that is proportional to the particle volume. The particle/liquid interface generally has a different conductivity than either the bulk liquid or bulk particle, usually higher. The conductivity of a particle is the sum of these volume and surface contributions; thus, the particle conductivity depends on the surface-to-volume ratio of the particle and usually increases with surface-to-volume ratio, that is, small particles of a given material are usually more conductive than large particles.

EXPERIMENTAL SECTION

Glass structures were designed and made in-house using standard photolithography techniques with glass substrates. The dielectrophoresis experiments were performed in a glass microfluidic circuit driven by a DC high-voltage source. Videos of the resulting motion of fluorescent polystyrene particles and *E. coli* were taken using a digital video camera mounted on an inverted epifluorescence microscope.

Apparatus. A schematic representation of the equipment used is shown in Figure 1. Experiments were conducted in a microfluidic chip consisting of patterned channels isotropically etched 10-μm deep in glass with a thermally bonded glass cover. The microfluidic chip was reversibly sealed to a test fixture via a vacuum chuck. This PDMS fixture provided 16 open reservoirs (Figure 1a). A high-voltage power supply (Stanford Research Systems, PS350, Palo Alto, CA) was used to apply electric fields by employing platinum-wire electrodes with a 0.5-mm diameter (Omega Engineering INC., Stamford, CT). The DEP behavior of cells and inert particles were imaged by an inverted fluorescence microscope (model IX-70, Olympus, Napa, CA) using a live/dead assay filter set (Chroma Technologies Corp, Brattleboro, VT). The data were collected in the form of videos that were captured from a Sony digital camera (Sony, San Diego, CA) using a program written in-house. Figure 4c was taken with a MacroFire digital camera (Optronics, Goleta, CA). The cells were labeled using a standard live/dead bacterial nucleic acid stain assay, Syto 9 and propidium iodide (Molecular Probes, Eugene, OR). The excitation/emission maximums for these dyes are 480/500 nm for Syto 9 and 490/635 nm for propidium iodide. Syto 9 is a green fluorescent dye that penetrates live and dead cells. Propidium iodide is a red fluorescent dye that penetrates only cells having a damaged membrane (such as heat or chemically treated, nonviable cells). If both dyes are present in a dead cell, the signal from the propidium iodide dominates and the dead cell fluoresces red. Carboxylate-modified polystyrene microspheres, FluoSpheres, (Molecular Probes, Eugene, OR) having a density of 1.05 mg/mm^3 and diameters of 200 nm and 1 μm were utilized without further modification.

Microfluidic Circuit Fabrication. The microfluidic chip contained 12 sets of independently addressable subcircuits. Each subcircuit was straddled by two liquid reservoirs and consisted of six separate patterned microchannels (Figure 1a). The length of the microchannels was 10.2 mm. Different post geometries were studied (squares, triangles and circles). The insulating posts spanned the entire depth (10 μm) of the microchannel (Figure 1b). The best results were obtained with microchannels with uniform square arrays of circular posts at different angles with respect to the applied electric field.

The microchips were fabricated from Schott D263 glass wafers (100-mm diameter, 1.1-mm thick, S. I. Howard Glass Company, Worcester, MA) using standard photolithography, wet etch, and bonding techniques. The photomasks were designed using DW-2000 (Design Workshop Technologies., Montreal, Canada) and fabricated by Photo Sciences Inc., (Torrance, CA). D263 borosilicate wafers were sputter-deposited (Cooke Vacuum Products., South Norwalk, CT) with chromium metal to a thickness of 200 nm, which served as the hard mask. A 7.5-μm-thick layer of SJR 5740 (Shipley Corporation, Marlborough, MA) positive photoresist was spin-coated on the wafer and soft-baked at 90 °C for 5 min. The mask pattern was transferred to the photoresist by exposure to UV light in a contact mask aligner at 775 μJ/mm^2. Exposure time varied depending on flux intensity (MA6, Karl Suss America Inc., Waterbury Center, VA). After exposure, the photoresist was developed with Microposit developer concentrate (Shipley Corporation, Marlborough, MA) and hard-baked for 30 min at 125 °C. Exposed chromium was etched with CEN 300 Micro-chrome etchant (Microchrome Technologies Inc., San Jose, CA). The subsequently exposed glass was etched with a 16% HF solution (Shape Products Company, Oakland, CA), and the remaining chrome was removed. Via access holes were drilled in the cover plate (D263 Glass) with diamond-tipped drill bits (Amplex, Worcester, MA). The etched wafers and drilled cover plates were cleaned with 4:1 H_2SO_4/H_2O_2 (100 °C) and destressed with 1% HF solution. The substrates were then immersed into an 80 °C 40% NaOH solution, rinsed in a cascade bath, spun dry, aligned for contacting, and thermally bonded by slowly ramping the temperature to 610 °C for 5 h in a nitrogen-purged programmable muffle furnace (model 48000, Thermolyne, Dubuque, IA). The standard chips were diced with a programmable radial arm saw (model 7100AD, Kulicke and Soffa., Willow Grove, PA) into individual devices.

Experiment Preparation. Before each experimental session, it was necessary to eliminate any organic materials deposited in the microchannels. These materials were eliminated by ashing the device in a programmable muffle furnace (model 48000, Thermolyne, Dubuque, IA), slowly ramping temperature to 500 °C for 5 h. The reservoir openings in the chip were aligned with

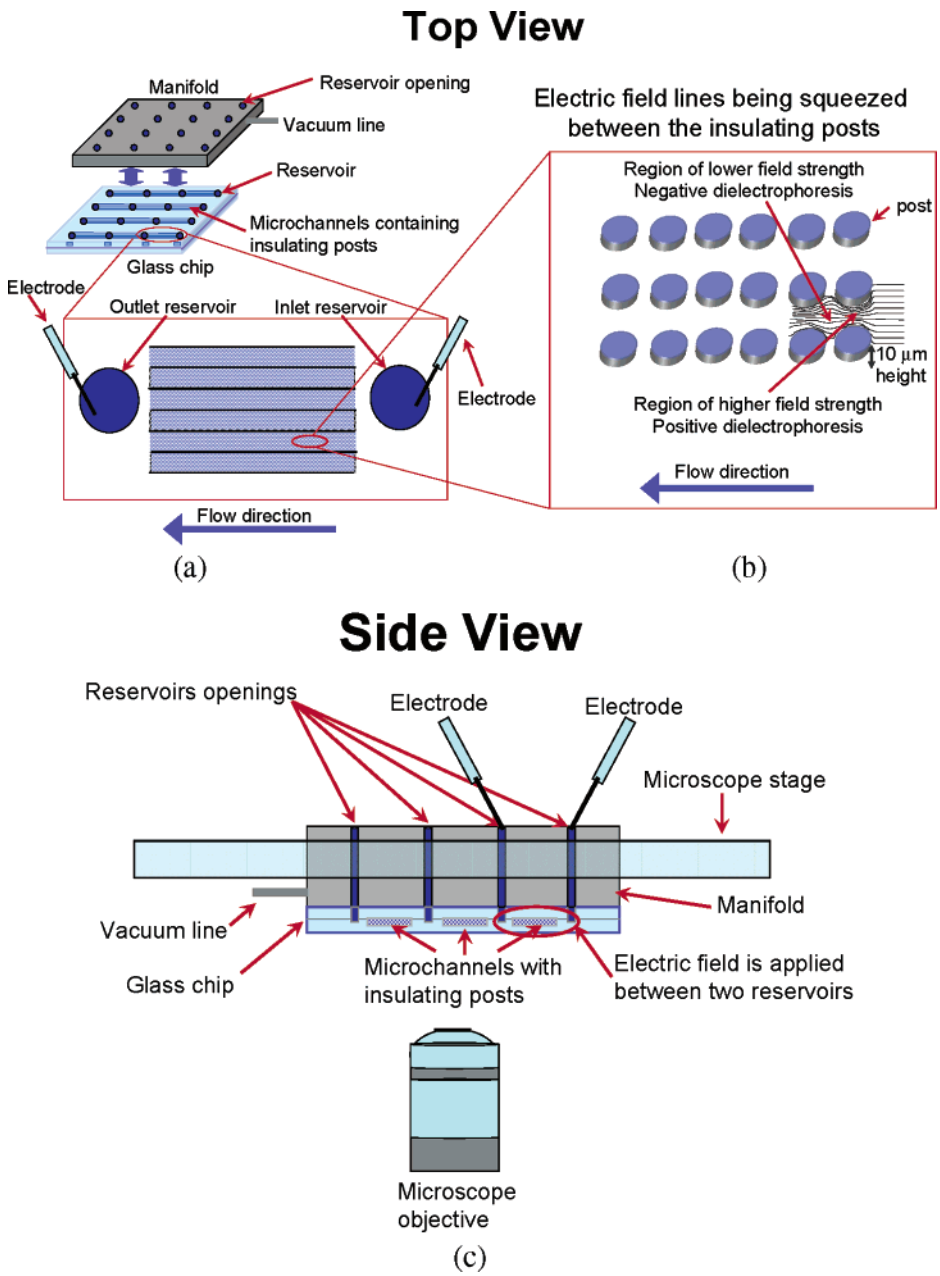

Figure 1. Schematic representation of the experimental setup: (a) top view, showing the manifold, glass chip, an enlargement of the flow microchannels; (b) cartoon showing the electric field lines being squeezed between the insulating posts; (c) side view showing the manifold and glass chip on the microscope stage.

the manifold (Figure 1c), and the desired channel and corresponding reservoirs were filled with deionized water. The pH of the DI water was measured at the inlet and the outlet reservoirs before and after running the experiments, and a pH change of 1 unit or less was observed. Care was taken to eliminate pressure-driven flow produced by liquid-level differences in the reservoirs. A sample of labeled cells, inert polystyrene carboxylate-modified particles, or both was introduced at the inlet reservoir. Electrodes were placed at the inlet and outlet reservoir, and an electric field was applied across the microchannel (10.2 mm long) containing the insulating-post structures. The dielectrophoretic behavior of the cells and particles was recorded by employing the microscope and video camera.

Cell Lines/Labeling Protocols. Lyophilized *E. coli* (cell strain BL21) was obtained from Stratagene (La Jolla, CA) and grown in LB nutrient broth. Cultures were grown overnight at 37 °C in an incubator to achieve saturation conditions. A 1:10 volumetric dilution of the cell culture was then allowed to grow in the LB liquid broth into late log phase to a cell concentration of 6×10^8 cells/mL, verified by OD measurements at 600 nm.[73] Cells were centrifuged at 5000 rpm for 10 min in order to eliminate the LB nutrient broth. Live cells were resuspended in DI water utilizing a vortex mixer. Dead cells were obtained by heating an aliquot of live cells for 20 min at 80 °C. Live and dead cells were then labeled with the Syto 9−propidium iodide live/dead BAClight bacterial stain (Molecular Probes, Inc., Eugene, OR) following the kit

(73) Ausubel, F. M.; Brent, R.; Kingston, R. E.; Moore, D. D.; Seidman, J. G.; Smith, J. A.; Struhl, K. *Short Protocols in molecular Biology*, 5th ed.; Wiley: New York, 2002.
(74) Green, N.; Morgan, H. *J. Phys. D: Appl. Phys.* **1997**, *30*, 2626−2633.

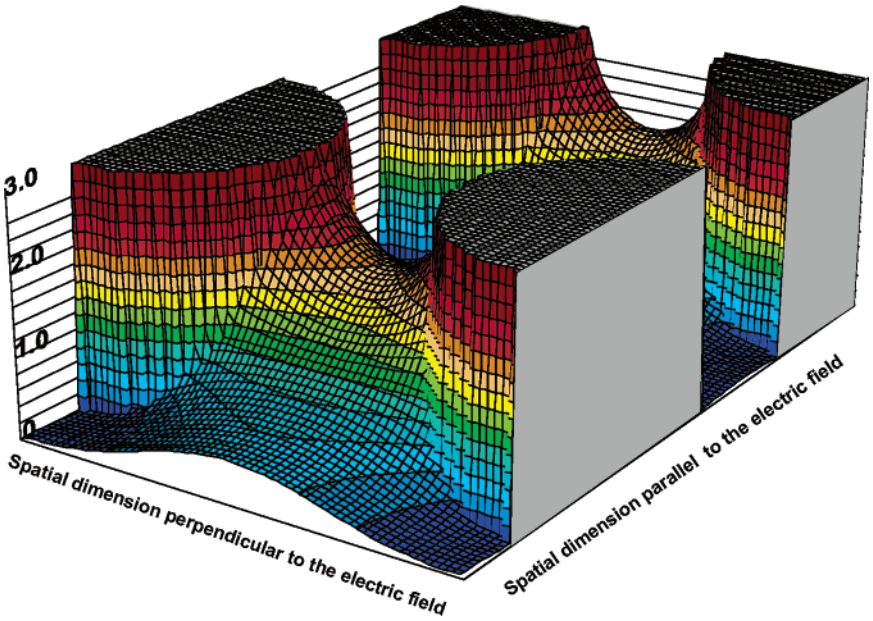

Figure 2. The variation of |**E**·**E**|, the electric field intensity, in an array of circular posts like in Figure 1b. The vertical axis shows the intensity normalized by the field intensity without the insulators. The peak concentration factor is ~3.02. By comparison, the theoretical field concentration factor for an individual circular post is 3. Flow direction is from left to right. The potential barrier between the posts traps the particles. The circular posts are 130 μm in diameter, 200 μm center-to-center, and at 0° with respect to the applied field.

instructions. For live cells, the Syto 9 labeling technique was utilized, whereas for the dead cells, propidium iodide was used. This produces live cells that will fluoresce green (excitation/emission 480/500 nm) and dead cells that fluoresce red (excitation/emission 490/635 nm), and allowes for distinct direct visualization. For every milliliter of cell culture present in the vial containing the live cells, 3 μL of the Syto 9 green-fluorescent nucleic acid stain was added. For every milliliter of the dead cell culture, 3 μL of the propidium iodide staining solution was added. The cells were then incubated at room temperature for 15 min. Both cell types were then concentrated by centrifugation at 5000 rpm for 10 min. The labeled cells were recovered by centrifugation at 5000 rpm for 10 min, washed three times with DI water to remove any free dye, and finally resuspended in DI water to the desired final volume to reach the appropriate cell concentration (typically 6×10^8 cells/mL). The DI water employed had a conductivity of 2.25 μS/mm, and the conductivity meter employed was a Mettler Toledo MC126 (Mettler Toledo, Columbus OH). These two cell cultures were then mixed to give varying concentrations of live/dead cells. A 50-μL portion of these cell cultures was added to the inlet reservoir in the flow manifold via pipet.

Safety Considerations. The use of high voltage is a hazard that requires training and safety measure, such as an interlocks and current-limiting features. Both the Syto 9 and propidium iodide labels were handled with care. All organisms used were Bio Safety Level 1 (BSL1). Care was taken to handle BSL1 materials and dispose of the waste according to the US Center for Disease Control and Prevention (CDC) guidelines and Sandia National Laboratories' policies.

RESULTS AND DISCUSSION

Electric Field Gradients with Insulating Posts. As eq 1 indicates, the dielectrophoretic force is of second order in the applied electric field. By applying an electric field across a microchannel containing insulating posts, an electric field gradient is obtained as a function of the post size and geometry.[2] Figure 1 shows the iDEP manifold and chip with a schematic representation of the electric field lines being squeezed between the insulating posts shown in Figure 1b. Figure 2 shows the variation of the dimensionless electric field intensity ($\mathbf{E}^2 = \mathbf{E}\cdot\mathbf{E}$) produced by the array of insulating posts. The values of $\mathbf{E}^2$ illustrated in the figure were normalized by the field intensity ($\mathbf{E}^2$) without the insulators. The peak concentration factor was ~3.02, that is, the field intensity was increased 3-fold by the presence of the insulating posts. As Figure 1 indicates, the electric field intensity is higher at the narrow spaces between the posts, like in the schematic representation of the field lines shown in Figure 1b. The dielectrophoretic potential barrier between the posts traps the particles. The data presented in Figure 2 was obtained by employing a potential flow solver called Laplace. The assumed ideal electrokinetic flow field is solved directly from the Laplace equation ($\nabla^2\phi = 0$) that describes the electric potential and fluid velocity potential without solving the coupled momentum transport (Navier−Stokes) and Poisson equations. More information about the Laplace solver can be found in Cummings and Singh.[2]

Live *E. coli*. Figure 3 shows the concentration of live *E. coli*, a Gram negative bacterium (stained green), obtained by applying iDEP. Figure 3a shows the cells in the microchannel filled with insulating posts (circular posts) before applying the electric field. In the absence of an electric field, the cells do not move. Figure 3b and c shows the trapping of *E. coli* when fields of 120 and 160 V/mm, respectively, are applied. From the figures, it can be noted that *E. coli* is not trapped in the regions of higher field intensity (the narrowest space between the circular posts). At the lower electric field (120 V/mm, Figure 3b) the cells are trapped closer to the region of higher field intensity. When the electric field is

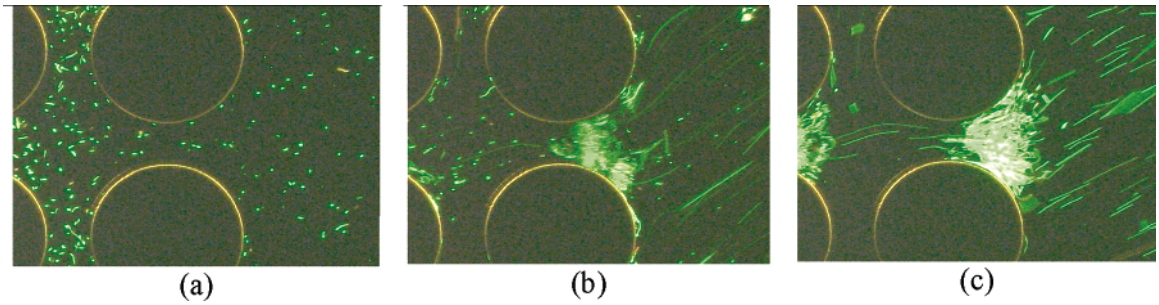

Figure 3. Concentration of live *E. coli* by using iDEP, 10× magnification, inverted fluorescence microscope. Live *E. coli* cells are labeled green (Syto 9, Molecular Probes, Eugene, OR) at a concentration of 6×10^7 cells/mL. Flow direction is from right to left. The background electrolyte is deionized water. The circular posts in the array are wet-etched in glass 10-μm tall, 200-μm in diameter, and on 250-μm centers and at 0° with respect to the applied field. The electric fields are (a) 0 V/mm no concentration of cells; (b) 120 V/mm, concentration of cells; and (c) 160 V/mm, high concentration of cells.

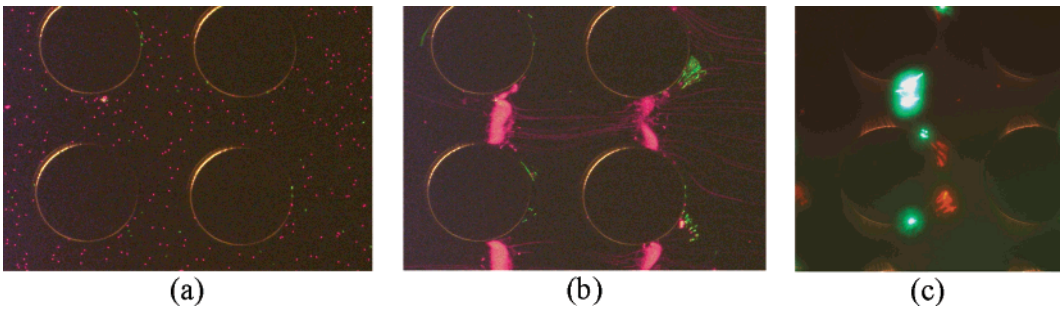

Figure 4. Simultaneous concentration and separation of live *E. coli* (green) and inert 1-μm red carboxylate-modified polystyrene particles and dead *E. coli* (red) and inert 1-μm green carboxylate-modified particles by using iDEP. All conditions are as in Figure 3, except the live cells are at a concentration of 6×10^6 cells/mL and the 1-μm polystyrene beads are at a concentration of 3.6×10^9 beads/mL. The circular posts in (a) and (b) are 10-μm deep, 150-μm in diameter, on 250-μm centers, and at 0° offset. For (c), the center-to-center dimension is 200 μm. The electric fields applied are (a) 0 V/mm, no concentration of live cells or particles; (b) 200 V/mm, high concentration and differential trapping of cells (negative DEP) and particles (weakly negative DEP); and (c) 40 V/mm, differential DEP trapping of dead cells and carboxylate-modified particles.

increased (160 V/mm, Figure 3c), the cells are more repelled from the region of higher field intensity. This indicates that under the current operating conditions, live *E. coli* exhibits negative DEP. These results agree qualitatively with the values of the CM factors shown in Table 1. The CM factor for the membrane of live *E. coli* cells is −0.5, which means that live *E. coli* exhibits negative DEP under DC electric fields. As described previously, under a DC electric field, the conductivity of the cell membrane is the dominant factor in the DEP of the cells. The behavior shown in Figure 3c also illustrates the capability of iDEP for cell concentration, since a large number of cells are trapped in a small volume of the glass chip. As mentioned above, a sample of *E. coli* was introduced into the inlet reservoir, then a flow was generated by applying the electric field. The deionized water passed through the array of insulating posts, but the cells present in the water were retained between the posts due to the dielectrophoretic trapping.

***E. coli* and Inert Polystyrene Particles.** Because of the potential of iDEP as a front-end method for bacterial analysis in water, it was important to determine the behavior of *E. coli* in the presence of inert, noncellular particles of size similar to the bacteria that could be in a sample background. Therefore, the behavior of bacteria with DEP was evaluated in the presence of polystyrene particles. The images obtained by applying iDEP to live *E. coli* and 1-μm carboxylate-modified polystyrene particles (shown in red) are presented in Figure 4. Figure 4a shows the cells and particles before the electric field had been applied. Figure 4b shows the steady-state DEP behavior when an electric field of 200 V/mm is applied. From this Figure, it can be observed that the polystyrene particles exhibit less-negative dielectrophoretic behavior, since they are trapped closer to the region of higher field intensity than the *E. coli*. Figure 4c shows differential DEP trapping of dead cells and 1-μm carboxylate-modified particles when a field of 40 V/mm is applied. The carboxylate-modified particles apparently exhibit a weakly negative DEP behavior, while the dead cells exhibit a strong negative DEP behavior. The cells in Figure 4b (live cells) and 4c (dead cells) are being repulsed from the regions of high field intensity, since the inert particles exhibit positive DEP and the cells are negative DEP. The bacterial results are in agreement with the values of CM factors shown in Table 1 for the membrane of live cells. Although 200-nm polystyrene particles are observed here to exhibit positive DEP, 1-μm polystyrene particles exhibit weak negative DEP, in conflict with the factor in Table 1. This trend probably reflects the varying relative importance of surface and volume conduction effects over this size range. In summary, this simple experimental system achieves differential trapping of cells and particles demonstrating the potential of iDEP for cell/particle discrimination and concentration.

Figure 5 shows the results of introducing a mixture of live *E. coli* and 200-nm inert carboxylate-modified polystyrene particles into the system. Figure 5a shows the behavior at an applied electric field of 200 V/mm. As observed in Figure 5a, a significant quantity of the *E. coli* was trapped at the first row of insulating

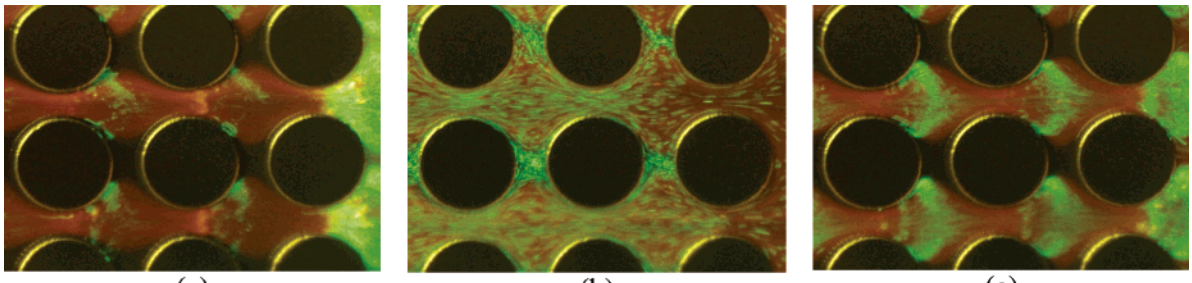

Figure 5. Simultaneous concentration and separation of live *E. coli* and inert 200-nm red carboxylate-modified particles by using iDEP. All conditions are as in Figure 3, except that 200-nm polystyrene beads are at a concentration of 4.6×10^{11} beads/mL. The circular posts in the array are 10-μm deep, 120-μm in diameter, on 200-μm centers, at 0° offset. The electric fields applied are (a) 200 V/mm, high cell concentration and trapping at the first row of insulating posts, while 200-nm particles do not trap; (b) 0 V/mm release of *E. coli* cells from dielectrophoretic trapping; and (c) retrap of cells at 200 V/mm. Cells are retrapped and concentrated at the first, second, and third rows, while 200-nm particles do not trap.

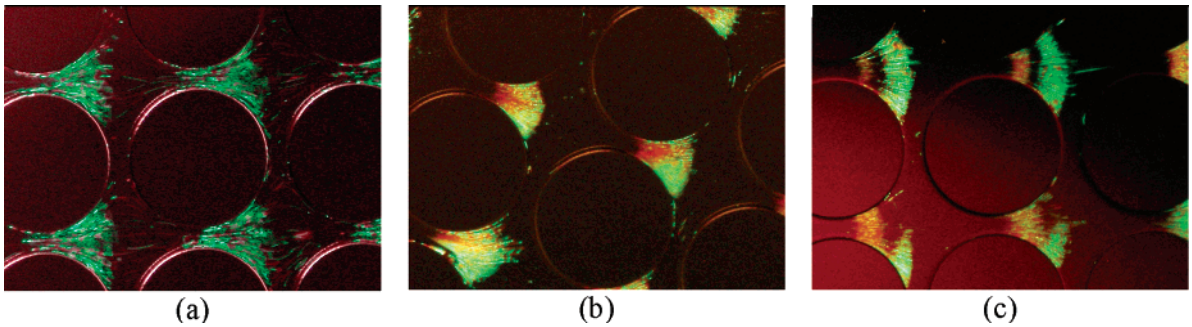

Figure 6. Simultaneous concentration and separation of live (green) and dead (red) *E. coli* by using iDEP. All conditions were as in Figure 3, except that dead cells were at a concentration of 6×10^7 cells/mL and labeled with propidium iodide (red dye, Molecular Probes, Eugene, OR). The circular posts in the arrays are 10-μm deep, 200-μm in diameter, on 250-μm centers, at 0° offset in (a) and (c), and 20° offset in (b). The electric fields applied are (a) 16 V/mm, only live cells are trapped; (b) 40 V/mm, differential banding on live and dead cells is observed; and (c) 60 V/mm, differential trapping of live and dead cells is shown by two separate bands of different color. Live cells (green) are trapped at the wider regions between the circular posts (negative DEP), and dead cells (red) exhibit less negative DEP, since they are trapped at the narrower regions between the circular posts.

posts. As the DEP traps at a row saturating with cells, some cells leak and are trapped at the downstream rows. Due to the small size of the 200-nm inert particles, they are not immobilized by dielectrophoresis at the applied electric field (200 V/mm). Equation 1 indicates that the dielectrophoretic force acting on a particle scales with the particle volume. Therefore, particles as small as 200 nm in diameter are typically not trapped under the current operating conditions. Figure 5b shows the release of live *E. coli* when the electric field of 200 V/mm was removed. It can be seen that the trapping of the cells was due solely to the applied electric field through DEP. Figure 5c shows that live *E. coli* was trapped again when the electric field of 200 V/mm was reapplied after the release. Due to the previous release, the cells were able to reach positionsfarther into the array of insulating posts; that is, cells were trapped in significant amounts in the second and third rows of insulating posts. In Figure 5a, most of the trapping was observed only at the first row.

From Figure 5c, it can be observed that the cells trap in two distinct bands. The majority of the cells exhibit negative DEP behavior, since they are trapped far from the areas of higher field strength. A small portion of the cells exhibit a less negative DEP behavior, since they are trapped closer to the regions of higher field strength. It was suspected that these latter cells were dead, and therefore, their DEP behavior changed. To prove this hypothesis, a new set of experiments was carried out using live and dead cells that were labeled using a standard live/dead fluorescent assay.

Live and Dead *E. coli*. A mixture of live and dead *E. coli* was introduced into the system and differential trapping was observed. Figure 6 shows the results obtained with live and dead *E. coli*. The live cells are labeled with a green dye, and the dead cells are labeled with a red dye. Figure 6a shows live cells exhibiting trapping DEP, while dead cells exhibit streaming DEP at an applied field of 16 V/mm. At this low applied electric field, only live cells are trapped, while dead cells are able to pass through the array of insulating posts. From Table 1, it can be observed that the values of the CM factors for live and dead cells under a DC electric field are negative (values for the cell membrane). This means both live and dead cells will exhibit negative DEP behavior. In addition, from Table 1, it can be seen that the magnitude of the CM factor for a live cell is greater than that of a dead cell. Because the electrokinetic mobility of the live and dead cells is observed to be nearly identical (consistent with previous reports[9]) and the size of the live and dead cells is nearly identical, the influence of the different membrane conductivities on the CM factor explains why live cells are trapped at lower applied electric fields than dead cells.

Figure 6b shows differential color-banding of the cells is observed at an applied field of 40 V/mm. The dead cells are concentrated closer to the narrowest space between the posts,

and the live cells are concentrated closer to the wider area between the posts. By increasing the applied electric field to 60 V/mm (Figure 6c), it is possible to observe two separated bands of trapped cells. A red band is made from the dead cells and a green band formed by the live cells. These results show true separation between live and dead cells. As for the few green cells present in the red band, it is believed that those cells are not viable, but since they were present in the sample of live cells, they were labeled green. From this figure, it can be observed that the band of dead cells is trapped in regions of higher field intensity, closer to the narrowest spaces between the circular posts. The live cells exhibit the same negative DEP observed previously. As predicted by the factors in Table 1, these results show that *the dead cells exhibit less negative DEP than live cells.*

Again, the difference in the response of the dead and live cells arises from the differences in the conductivities of their cell membranes ($\sim$1 and $\sim 10^{-4}$ μS/mm, respectively).[31] Because a DC electric field was applied in these experiments, the conductivity of the cell membrane was the dominant factor determining the dielectrophoretic response of the cells. Dead cell membranes are expected to have generally higher conductivities than live cell membranes.[31] As discussed above, when a cell dies, the cell membrane becomes permeable, and its conductivity increases significantly. By having a more conductive cell membrane, dead cells exhibit less negative dielectrophoresis than live cells at low applied field frequencies, a prediction that is confirmed by the results presented in Figure 6c.

Because trapping occurs in the presence of electrokinesis, the possible contribution to apparent dielectrophoretic trapping due to differences in the electrophoretic mobility between the live and dead cells must be considered. In this system, under the conditions specified in this work, apparent electrokinetic velocity is the sum of the electrophoretic velocity and the electroosmotic flow. At low field strengths where electrokinesis dominates, it has been directly observed that the apparent velocities of the two types of bacteria are indistinguishable. This is most likely due to the magnitude of the electroosmotic flow compared to the relatively small differences in the electrophoretic mobility between the live and dead cells.

This observation is supported by the reports of cell separations by CE. The determination of the electrophoretic mobility of bacterial cells has been the focus of several studies. It has been found that the μ_{EP} of bacteria depends on surface softness, structure and charge, and cell age, as well as ionic concentration and pH of the running buffer.[19,23,24] Armstrong et al.[8−13,25] have analyzed microorganisms using electrokinetic techniques. In the CE method for the determination of cell viability for *B. infantis*, *L. acidophilus*, and *S. cerevisiae*, peaks of live and dead cells had essentially the same migration times, indicating the same electrophoretic mobility.[9] Identical migration times were also obtained for live and dead *L. acidophilus* cells from commercial tablets.[10]

Several studies found that the electrokinetic mobility of bacteria is mainly controlled by the EOF. This means that the μ_{EP} is minimal when compared with the EOF.[11,12,18,24] Li and Harrison[18] stated that in uncoated glass chips, the solvent mobility due to EOF is greater than the electrophoretic mobility of bacteria. The work cited above is consistent with the direct observation of the cell velocities in our laboratory. Both the laboratory observation and the cited work support the conclusion that the differences in the conductivity between the live and dead cells reflected by their respective CM factors explain the iDEP selectivity in these experiments.

CONCLUSIONS

The application of insulator-based (electrodeless) dielectrophoresis (iDEP) for the manipulation of bacteria and inert particles has been demonstrated. This is the first report of iDEP trapping and manipulation of live and dead bacteria. A nonuniform electric field was generated by applying a DC electric field across a microchannel filled with insulating posts. Regions having higher field intensity were generated in the narrowest spaces between the insulating posts.

Differential dielectrophoretic trapping of live *E. coli* in the presence of dead *E. coli* and inert polystyrene particles was demonstrated. Live *E. coli* exhibited negative dielectrophoresis, that is, they were repelled from regions of high electric-field intensity. Concentration of *E. coli* was qualitatively observed as result of the reversible trapping. Inert 1-μm polystyrene particles exhibited a weaker negative DEP behavior, because they were less strongly repelled from regions of high field intensity. Differential trapping of 1-μm particles and live *E. coli* was observed. Because of their small volume and large electrokinetic mobility, the 200-nm polystyrene particles are trapped at a higher electric field than was applied in the bacteria experiments. When applying iDEP to a mixture of live and dead *E. coli*, it was observed that dead cells exhibit less negative DEP than live cells, since dead cells have a more conductive cell membrane than live cells.

These results illustrate the great potential of iDEP for the selective concentration of bacteria and particles. An iDEP device can be envisioned as a front-end device for bacterial detection and concentration in water. Future work on iDEP can be expected for a number of applications including water and biomedical analysis.

ACKNOWLEDGMENT

This work was performed by Sandia National Laboratories for the United States Department of Energy under Contract DE-AC04-04AL85000. It was funded by the Laboratory Directed Research and Development Program of Sandia National Laboratories. The authors are grateful to Joanne Volponi and Camille Troup for their assistance in preparing and labeling cells. The authors thank Boyd Wiedenman and Allen Salmi for technical assistance in the fabrication of the chips and manifold.

Received for review July 15, 2003. Accepted January 12, 2004.

AC034804J